RESOURCE GEOLOGY, vol. 56, no. 2, 133–140, 2006

Synthetic Fluid Inclusions in the Systems NaCl-H_2O and NaCl-CO_2-H_2O: Dissolution Temperatures of Halite

Hiroki NAGASEKI and Ken-ichiro HAYASHI*

Department of Mineralogy, Petrology, and Economic Geology, Graduate School of Science, Tohoku University, Sendai 980-8578, Japan [e-mail: nagaseki@ganko.tohoku.ac.jp]
* *Doctoral Program in Earth Evolution Sciences, Graduate School of Life and Environmental Sciences, University of Tsukuba, Tsukuba 305-8572, Japan*
Received on September 25, 2005; accepted on February 2, 2006

Abstract: This study examined the effect of CO_2 on NaCl solubility in hydrothermal fluid, with the synthetic fluid inclusion technique. Fluid inclusions of 30-40 wt% NaCl and 5 mol % CO_2 were synthesized, and their halite dissolution temperatures, T_m(halite), were measured. The solubilities of NaCl in CO_2-bearing aqueous fluid were obtained at 160-320°C under vapor-saturated pressures. The T_m(halite) value in aqueous fluid with 5 mol % CO_2 obtained in this study agrees with that of Schmidt et al. (1995), showing that 5 mol % CO_2 reduces the solubility of NaCl by about 1 wt%.

Calculation of magnetite solubility suggests that 5-10 mol % CO2 decreases magnetite solubility by 4.5-8.9 % relative to the magnetite solubility in CO2-free solution. Therefore, an increase of CO2 content in ore-forming solutions may cause deposition of iron minerals and produce ore deposits.

Keywords: halite solubility, synthetic fluid inclusion, effect of CO_2, NaCl-CO_2-H_2O system

1. Introduction

Hydrothermal fluid in the system NaCl-CO_2-H_2O is widely distributed in the earth's crust. It includes hydrothermal ore-forming fluid (e.g., Dugdale and Hagemann, 2001; Wang et al., 2004), volcanic fluid (e.g., Chiodini et al., 2001), metamorphic fluid (Fu et al., 2001), carbonatite-related fluid (e.g., Genge et al., 2001), and submarine hydrothermal system (e.g., Kelley and Früh-green, 2001). Although NaCl solubility in water above 100°C has been reported by many studies (e.g., Benrath et al., 1937; Keevil, 1942; Potter et al., 1977; Chou, 1987; Sterner et al., 1988), the effect of CO_2 on NaCl solubility at elevated pressures is not well understood. Recently, Schmidt et al. (1995) and Schmidt and Bodnar (2000) have suggested that 5 or 10 mol % CO_2 in the ternary fluid lowers NaCl solubility by 1 or 2 wt% at 320°C. Shmulovich and Graham (1999) have estimated the halite-saturated field in the phase diagram of the H_2O-CO_2-NaCl system at 800°C and 900 MPa by the interpolation of experiments.

Because the halite solubility curve in the presence of CO_2 has not been established, researchers have ignored the effect of CO_2 on salinity in discussions about hydrothermal fluid. Thus, by measuring the NaCl solubility curve we will make it possible to expand and improve equations of state for the system NaCl-CO_2-H_2O (e.g., Bowers and Helgeson, 1983; Bakker, 1999; Duan et al., 1995; Duan and Sun, 2003) and we will be able to describe the history and/or the behavior of hypersaline fluid more precisely. The purpose of this study is to evaluate the effect of CO_2 on NaCl solubility in hypersaline hydrothermal fluid using an experimental approach.

The NaCl solubility in CO_2-bearing hydrothermal solutions is also useful for microthermometric measurement of salinity in fluid inclusions. Hypersaline fluid inclusions usually contain a halite daughter crystal at room temperature when the NaCl concentration is >26 wt%. In this case, salinity has been estimated from the NaCl dissolution temperature, T_m(halite), measured by means of a heating stage. Thus, the present study contributes to estimate the salinity more precisely when CO_2 concentration is known.

In order that compositions of the fluid in synthetic inclusions may be consistent with starting composition, inclusion syntheses should be carried out within the single-phase region in the phase diagram shown in Figure 1. Frantz et al. (1992) have determined the immiscibility field and the compositions of coexisting immiscible fluids for the NaCl-CO_2-H_2O ternary system at 500-700°C and 100-300 MPa. According to that, we decided to synthesize fluid inclusions at 500°C and 110 MPa total pressure, with solution whose compositions is 30-40 wt% NaCl and 5 mol % CO_2 plotted in Figure 1, in order to evaluate NaCl solubility in the system CO_2-H_2O.

2. Experimental Section

The synthetic fluid inclusion technique (Sterner and Bodnar, 1984) is employed in this study. This technique makes it possible to sample high P-T fluid without cooling or depressurizing, and thereby to minimize changes after the experiments, such as oxidation by the air or cont-

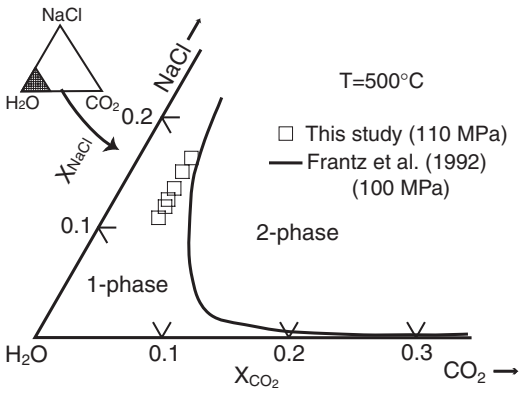

Fig. 1 Experimental compositions for the measurement of halite solubility in CO_2-bearing hydrothermal solutions. In the figure, each open square corresponds to a single run. The solid curve denotes the 1-phase/2-phase boundary at 100 MPa from Frantz et al. (1992).

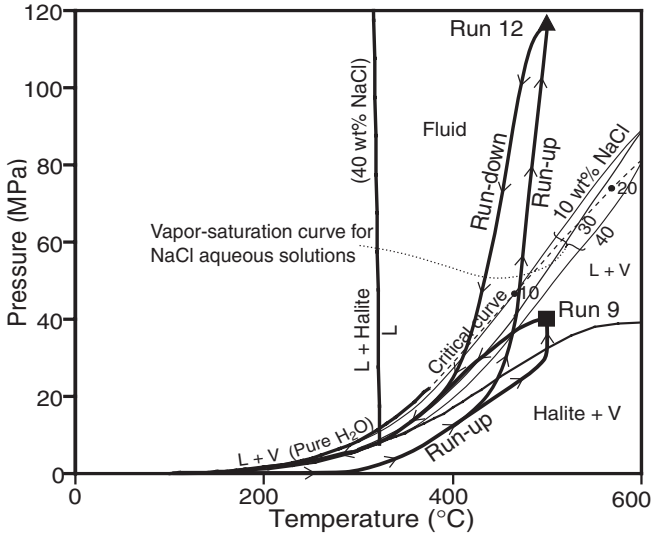

Fig. 2 Typical examples of P-T paths during run-up and run-down of the experiments. In the figure, lines show the P-T paths from the room temperature to experimental P-Ts shown in a square or a triangle and vice versa. P-T values of the path could be less accurate than experimental P-T because measuring device could not attain the equilibrium with actual P-T. The halite solubility curve and the critical curve of H_2O-NaCl fluid are from Bodnar (1994) and Knight and Bodnar (1989), respectively. The vapor-saturation curves for H_2O-NaCl fluid are derived from Bischoff (1991), Sourirajan and Kennedy (1962) and Bodnar et al. (1985). 3-phase (L + V + Halite) curve is from Keevil (1942) and Bischoff (1991). Vapor-saturation curve for pure H_2O is from Wagner and Pruß (2002).

amination. In recent years, this technique has been applied for many experimental studies of aqueous fluid (e.g., Sterner et al., 1988; Knight and Bodnar, 1989; Frantz et al., 1992; Hanley et al., 2005).

2.1. *Experimental apparatus*

A Hastelloy C276 high P-T pressure vessel with inner volume of 21 cm^3 was used in this study. Temperature and pressure limits of this vessel were 600°C and 140 MPa, respectively. Several heater rods (heating rate: about 8°C/min) embedded in the autoclave body were used for heating, and chromel-alumel thermocouples were used for temperature control and measurement. Temperature was controlled by a digital temperature controller (Shimaden Co., Ltd.). Control and measuring thermocouples (K-type) were calibrated against the standard thermocouple which was calibrated to the freezing and boiling points of water, and melting point of NaCl. Experimental temperatures of this study were controlled within ±3°C. Pressure was measured by a Bourdon-tube pressure gauge (Yamazaki Keiki Mfg. Co., Ltd.) within the accuracy of ±1 MPa. A hand pump was used for pressurization by injecting water, and water was discharged for depressurization.

2.2. *Synthesis of fluid inclusions*

A natural quartz crystal was cut into rods of 4 mm × 4 mm × 2-3 cm. The quartz rods were heated overnight in an electric furnace at 1000°C to decrepitate any original fluid inclusions. Then, the rod was heated to 400°C for over 5 hours and dropped into distilled and deionized water to generate fractures. Then the rods were dried overnight in a vacuum desiccator to eliminate water from cracks. Water, NaCl, and silver oxalate (to produce CO_2; see below) as starting materials were weighed precisely and loaded into a gold tube (3-5 cm long, 6 mm in outer diameter, 0.2 mm in thickness) with a quartz rod and quartz powder. The accuracy of measuring starting material is ≤0.1mg. Then, both ends of gold tube were sealed by weld. Quartz powder was used as a source of silica to heal cracks that trapped the experimental solution. To verify that the ends of the tubes were completely welded, the gold capsule was kept in a vacuum desiccator for about 15 minutes and its weight before and after evacuation was compared. The gold capsule was loaded into the pressure vessel, and kept at 300°-600°C and 7-120 MPa for 3-14 days. In the period of keeping the P-T conditions, the fluctuation of temperature and pressure are <1°C and <1 MPa, respectively. After the experiment, the autoclave was cooled down to room temperature within about 30 minutes, using an air-ventilation fan. Typical P-T path of the run-up and run-down in this study is shown in Figure 2. Then, the quartz rod was pulled out of the gold capsule.

The quartz rod was cut and polished on both sides to prepare sections about a 0.25mm thick for microscopic observation. These sections were also examined in a Linkam® THMSG600 heating-freezing stage, which is calibrated with melting points of H_2O, metallic Sn (232.0°C), metallic Bi (271.3°C), and $NaNO_3$ (306.8°C). Accuracies of temperature control during heating experiments are ±0.2°C, and ±0.1°C for freezing points. Heating experiments and optical observations indicated that the

Table 1 Homogenization temperatures, dissolution temperatures of NaCl and ice melting temperatures of fluid inclusions synthesized in the system NaCl-CO_2-H_2O.

Run No.	Experimental conditions of synthesis				Homogenization temperature				Dissolution of NaCl				Ice melting temperature		
	T °C	P MPa	Salinity wt% NaCl	CO_2 mol%	T_h °C	σ °C	Homogenize to	n	T_m(NaCl) °C	Range (°C)	σ °C	n	T_m(ice) °C	σ °C	n
NaCl-H_2O system															
15	300	7	9.9	0.00	311.0	2.9	L & V	5	-	-	-	-	-7.0	1.8	2
16	300	7	29.9	0.00	306.6	8.0	L & V	4	-	-	-	-	-	-	-
1	500	81	30.0	0.00	456.0	6.5	L	7	-	-	-	-	-	-	-
3	500	83	10.0	0.00	413.2	0.0	L	2	-	-	-	-	-6.7	0.6	6
4	500	83	9.3	0.00	431.4	0.0	L	3	-	-	-	-	-	-	-
5	500	82	30.0	0.00	481.9	8.3	L	3	156.0	141.2-175.6	14.9	4	-	-	-
6	500	82	29.4	0.00	440.7	4.8	L	3	-	-	-	-	-	-	-
7	500	86	10.0	0.00	409.4	2.4	L	6	-	-	-	-	-7.1	0.2	6
8	500	86	50.0	0.00	475.0	16.7	L	11	433.5	377.9-450.9	29.1	7	-	-	-
9	500	40	10.0	0.00	519.3	10.3	L & V	13	-	-	-	-	-	-	-
10	500	40	29.9	0.00	507.8	8.1	L & V	10	-	-	-	-	-	-	-
11	500	117	10.0	0.00	374.0	3.9	L	7	-	-	-	-	-6.9	0.3	4
12	500	117	30.0	0.00	417.3	5.0	L	9	178.5	-	-	1	-	-	-
19	500	115	39.8	0.00	-	-	-	-	340.2	-	-	1	-	-	-
20	500	115	35.0	0.00	-	-	-	-	271.8	271.8-271.8	0.0	2	-	-	-
17	600	50	9.9	0.00	>600*	-	L & V	9	-	-	-	-	-	-	-
18	600	50	29.8	0.00	>600*	-	L & V	8	553.0	524.0-578.3	24.7	8	-	-	-
NaCl-CO_2-H_2O system															
21	500	100	5.9	3.82	398.5	3.4	L	4	-	-	-	-	-	-	-
22	500	100	20.0	8.88	405.9	1.6	L	4	-	-	-	-	-	-	-
24	500	50	20.0	9.09	493.8	1.3	L & V	5	338.4	336.3-340.0	1.6	8	-	-	-
27	500	100	40.0	4.97	459.8	6.2	L	5	331.4	320.5-336.8	6.6	7	-	-	-
28	500	100	39.9	8.79	503.8	1.3	L & V	5	374.4	374.0-375.0	0.5	6	-	-	-
29	500	50	39.9	5.01	500.9	3.9	L & V	7	398.3	397.8-398.6	0.5	3	-	-	-
30	500	50	40.2	10.12	-	-	L	-	445.2	435.9-454.9	9.0	10	-	-	-
31	500	117	30.0	5.00	502.7	0.5	L	2	166.0	161.5-171.4	3.3	9	-	-	-
34	500	113	37.7	4.95	-	-	L	-	317.6	316.5-318.4	1.0	3	-	-	-
39	500	110	35.0	5.02	-	-	L	-	271.0	266.8-276.0	2.8	7	-	-	-
40	500	110	33.2	5.05	-	-	L	-	240.8	238.9-242.2	1.3	6	-	-	-
43	500	113	31.9	4.96	-	-	L	-	217.7	216.8-218.8	1.4	2	-	-	-

Note. T_h: L+V→L or L+V→V; T_m(NaCl): Halite + L + V→L + V; T_m(ice): Ice + L +V→L + V
σ: standard deviation; n: number of measurements; -: not determined *:The upper limit of the heating stage; Vapor bubble was estimated to disappear at <610°C from the shrinking behavior of the vapor bubble.

fluid inclusions in the sections were not trapped during heating or cooling, but under the intended conditions, and the inclusions clearly trapped a homogenous fluid.

2.3. CO_2 source

Several previous researchers loaded gaseous CO_2 directly with gas pipette (Frantz et al., 1989) or used dry ice (Shmulovich and Plyasunova, 1993) as the CO_2 loading technique for gold capsule. In order to minimize the error of the CO_2 concentration, the silver oxalate ($Ag_2C_2O_4$) technique proposed by Sterner and Bodnar (1991) and Diamond (1992) was used in this study. Silver oxalate is handled easier than gaseous CO_2 or dry ice because silver oxalate is solid at room temperature. In previous studies, oxalic acid ($H_2C_2O_4$) was often used as a CO_2 source (e.g., Kotel'nikov and Kotel'nikova, 1990), but oxalic acid contains hydrogen atoms, and it may generate unexpected species such as water, carbon monoxide and hydrogen gas upon thermal decomposition (Holloway and Reese, 1974; Sterner and Bodnar, 1991).

Because silver oxalate reagent is not commercially available, it was synthesized from reagent grade oxalic acid and silver nitrate solutions according to the following reaction.

$$H_2C_2O_4(aq)+2AgNO_3(aq)\rightarrow Ag_2C_2O_4(s)+2NO_3^-+2H^+ \quad (1)$$

Silver oxalate decomposes at about 140°C (Holloway and Reese, 1974), and generates a stoichiometric amount of CO_2, 29.0 wt% of the silver oxalate loaded, by the following reaction (Krüger and Diamond, 2001).

$$Ag_2C_2O_4(aq) \rightarrow 2CO_2(g)+2Ag(s) \quad (2)$$

The completion of this reaction was checked prior to the hydrothermal experiments. The synthesized silver oxalate was heated and the amount of generated CO_2 was measured using a capacitance manometer. This confirmed that the CO_2 generation was stoichiometrically proportional to the mass of heated silver oxalate. Krüger and Diamond (2001) have suggested that the precipitation of chlorargyrite (AgCl) modified the salinity of the inclusion. How-

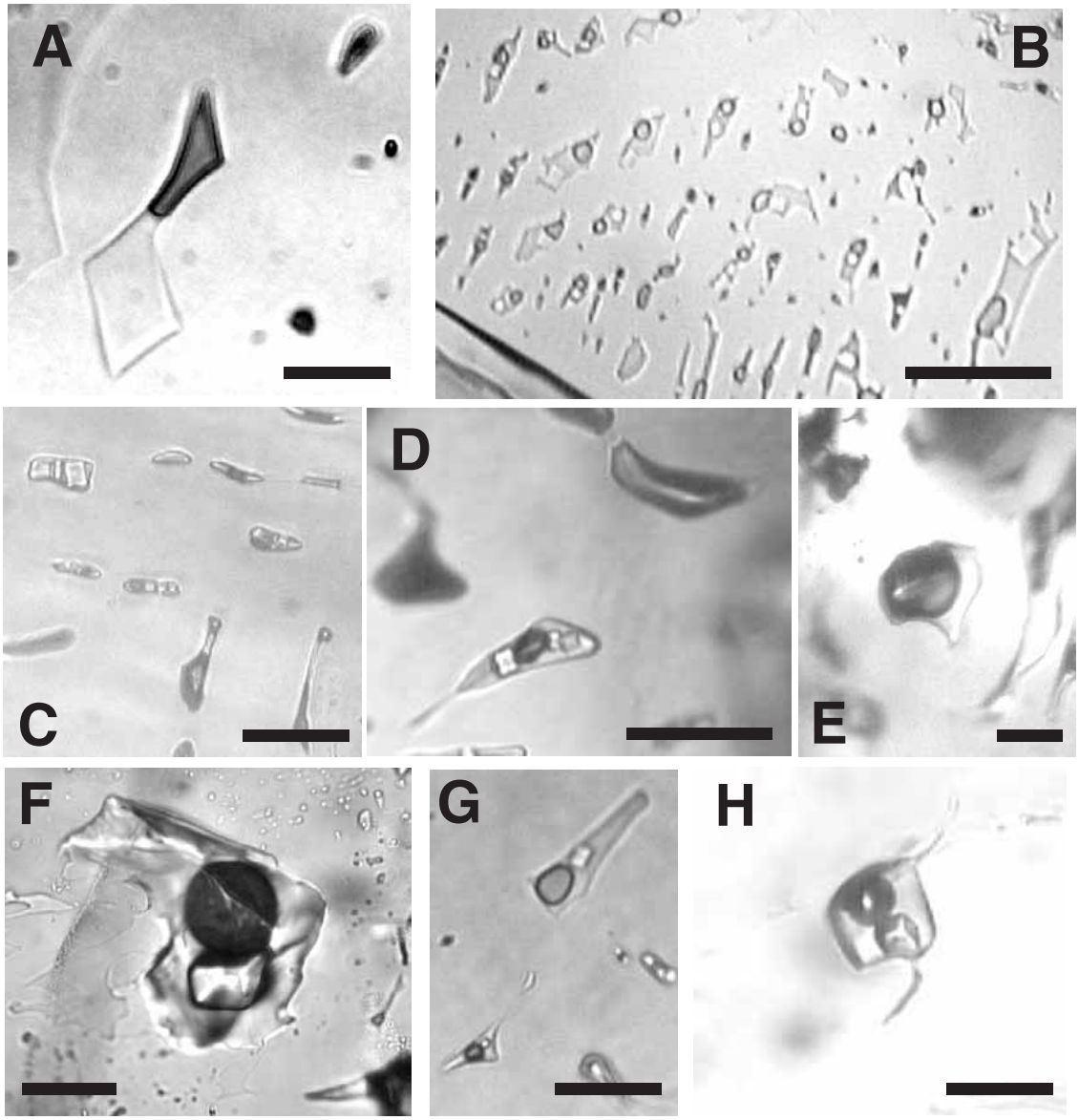

Fig. 3 Photomicrographs of fluid inclusions synthesized in this study. A: Flat two-phase inclusion (Run No. 4 at 500°C, 9.3 wt% NaCl). B: Irregular inclusions containing bubble and halite daughter crystal. Some of them suggest necking-down phenomena (Run No. 8 at 500°C, 50 wt% NaCl). C: Liquid-rich saline inclusions containing halite crystal and vapor-rich inclusions coexisting in a single sample (Run No. 18, 600°C, 29.9 wt% NaCl). D: Focused to a saline inclusion in the same sample as C. Note that two to three grains of halite are observed in brine inclusion. E: Focused to a vapor-rich inclusion in the same sample as C. F: Large irregular inclusion (Run No. 27, 500°C, 40 wt% NaCl). G: Poly-phase inclusion (Run No. 34, 500°C, 37.7 wt% NaCl). H: Isolated poly-phase inclusion with negative crystal shape (Run No. 43, 500°C, 31.9 wt% NaCl). Scale bars indicate 20 μm.

ever, no chlorargyrite daughter minerals were observed under an optical microscope and NaCl concentrations in this study is extremely high enough to negligible this effect. Therefore, this effect is not taken into consideration in the present study.

3. Results and Discussion

3.1. The system NaCl-H_2O

Seventeen runs were successfully completed in the system NaCl-H_2O. Synthesis conditions including temperature, pressure and NaCl concentration are summarized in Table 1. Photomicrographs of the synthetic inclusions are shown in Figure 3. Results of heating and freezing experiments of the fluid inclusions under the microscope are also shown in Table 1. The fluid inclusions synthesized at 500°C and 80-120 MPa homogenized to liquid during heating. Two syntheses were conducted at 600°C and 50 MPa (runs 17 and 18, Table 1). Inclusions in these runs trapped fluids in the 2-phase coexistence region, showing

brine inclusions containing halite crystal coexisting with gaseous inclusions at room temperature (see Fig. 3C, D and E). For inclusions trapped homogeneous aqueous fluid, the homogenization temperatures (T_h: L+V→L) were 18° to 90°C lower than the temperatures of the syntheses. It is because the T_h value of fluid inclusion is lower than the formation temperature in this condition (Sawaki et al., 1997). The pressure-corrected trapping temperature, using the isochore proposed by Zhang and Frantz (1987), agreed with the experimental temperature within 15°C.

Natural fluid inclusions of high salinity (>26 wt% NaCl) contain a halite daughter crystal at room temperature. However, synthetic fluid inclusions in this study with salinity between 26 and ~35 wt% NaCl did not contain a daughter crystal after the hydrothermal experiments. These fluid inclusions were cooled as low as the temperature of liquid nitrogen to precipitate halite crystal. For some runs, halite daughter minerals did not observe after this cooling because no halite crystals nucleated in the measured inclusion. In this case, inclusions containing two to three grains of NaCl are occasionally formed, and this may be caused by rapid crystallization of NaCl under very high supersaturation (see Fig. 3D).

As the temperature rose during the heating measurement, the NaCl daughter crystals dissolved in the fluid and then complete homogenization occurred by disappearance of the bubble. Dissolution temperatures of NaCl, T_m (halite), are shown in Table 1. The relation between T_m (halite) and the composition of the experimental solutions is plotted in Figure 4. The solubility curve of this study is compared with those of Keevil (1942), Potter et al. (1977) and Sterner et al. (1988) (Fig. 4). The mean of the T_m(halite) values agrees better with the studies by Keevil (1942) and Potter et al. (1977), but the large spread in values makes any comparison equivocal. In some runs, there are large uncertainties for the measurement of T_m (halite) because there might be a problem in the adjustment of the experimental equipment in the beginning of the study such as a position of a gold capsule in the autoclave.

3.2. *The system NaCl-CO_2-H_2O*

Prior to the determination of halite solubility, fluid inclusions were synthesized under conditions of 500°C, 50-110 MPa, 6-40 wt% NaCl, and 5-10 mol % CO_2 and the position of the immiscibility field for concentrated NaCl solutions was estimated. The microscopic observations at room temperature or the behavior of liquid and vapor during heating under the microscope indicate the phase state, 1-phase or 2-phase, under the conditions of the synthesis. Figure 5 plots the compositions of starting solutions and the phase states. When both liquid and vapor inclusions coexisted and halite daughter crystals

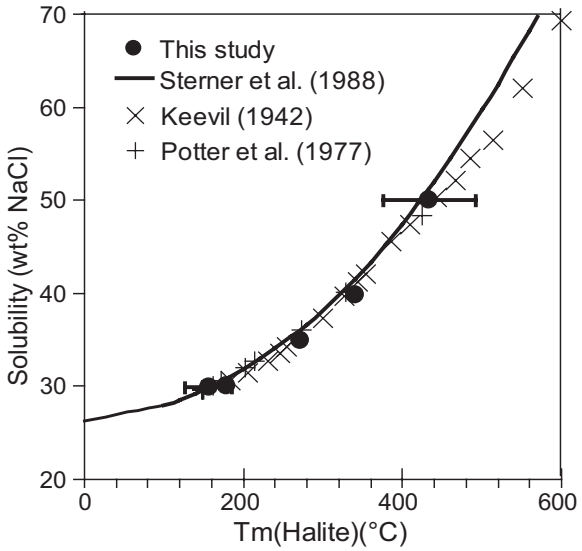

Fig. 4 Solubility of NaCl in the system NaCl-H_2O. Solubility is determined by measured value of T_m(halite) of halite daughter crystal. Data of this study are compared with those of Keevil (1942), Potter et al. (1977) and Sterner et al. (1988). The pressures of the data points shown in this diagram are those imposed by equilibrium between halite + liquid + vapor.

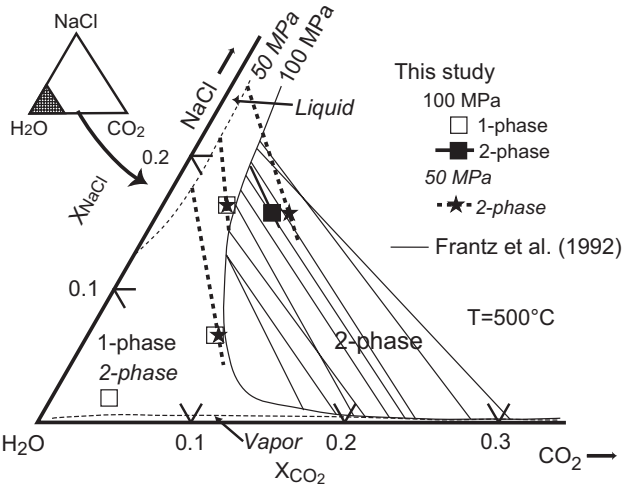

Fig. 5 Phase diagram for the system NaCl-CO_2-H_2O at 500°C, 50-100 MPa. The solid curves denote the 1-phase/2-phase boundaries at 100 MPa and the dotted curves show those at 50 MPa. The italicized explanations display the phase states at 50 MPa and the "tie-lines" representing the compositions of the coexisting liquid and vapor are given from the compositions of starting solution and the salinity obtained from fluid inclusion microthermometry.

were observed at room temperature, the salinity of the coexisting fluids was obtained by microthermometry and the position of "tie-lines" similar to Frantz et al. (1992) was determined. These results are consistent with Frantz et al. (1992) for <20 wt% NaCl. Figure 5 suggests that the solutions are in the 1-phase region under the experimen-

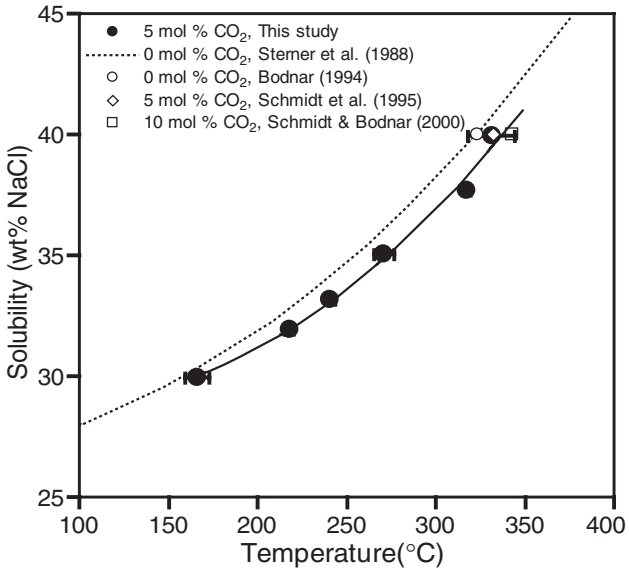

Fig. 6 Comparison of NaCl solubility curves obtained in this study with those of previous studies. This figure suggests that 5 mol % CO_2 lowers NaCl solubility by 1 wt%. The pressures of the data points shown in this diagram are those imposed by equilibrium between halite+liquid+ vapor. In the figure, "wt% NaCl" means the NaCl concentration of the solution in weight percent relative to H_2O.

tal conditions of this study.

The dissolution temperatures of the halite crystals, T_m(halite), of the fluid inclusions were obtained for samples synthesized at 110 MPa, 30-40 wt% NaCl and 5 mol % CO_2 from heating experiments under the microscope. Table 1 summarizes results of the microthermometry, and T_m(halite) of six runs in Table 1 are plotted graphically in Figure 6, because inclusions of these runs trapped homogeneous fluid and their compositions are equal to those of the experimental solutions. The best-fit regression line to data in Figure 6 is,

$$\text{Solubility (wt\% NaCl)} = 1.84\cdot10^{-4}\cdot(T_m(\text{halite}))^2 - 3.39\cdot10^{-2}\cdot(T_m(\text{halite})) + 30.61 \quad (3)$$

at temperatures between 160° and 330°C, pressure of 110 MPa, and 5 mol % CO_2.

Figure 6 compares the solubility of NaCl obtained in this study with those in the literature. In this study, some T_m (halite) values in CO_2-free conditions were also obtained, however, as mentioned in the "The system NaCl-H_2O" section, some runs have large uncertainties. Therefore, the values from published literature were adopted as those of CO_2-free conditions instead of those from this study. In the present study, Sterner et al. (1988) is applied as the T_m(halite) data in CO_2-free conditions because this is obtained from synthetic fluid inclusions, similar to the present study. It shows that halite solubility in CO_2-bearing water is lower by about 1 wt% than that in CO_2-free water (Sterner et al., 1988).

This study found that T_m(halite) =331.4°C in a fluid with 40 wt% NaCl and 5 mol % CO_2. This is in close agreement with the results of Schmidt et al. (1995). Schmidt and Bodnar (2000) have suggested that halite becomes about 1 % less soluble in 10 mol % CO_2-bearing water than compared to water with 5 mol % CO_2. This study shows that the solubility of NaCl systematically decreases as CO_2 concentration increases.

3.3. *Effect of CO_2 on mineralization*

The results of the present study suggest that CO_2 in hydrothermal fluid lowers NaCl solubility. To evaluate the effect of CO_2 on mineral solubility, a model calculation was conducted. Fluid inclusions with salinity >70 wt% are sometimes observed in hydrothermal ore deposits which are genetically related to magmatic water (Wilkinson, 2001). In particular, fluid inclusions with very high salinity are sometimes found in skarn type deposits. During skarn mineralization, CO_2 is produced by the reaction between carbonate and fluid, such as,

$$CaCO_3(s)+SiO_2(aq) = CaSiO_3(s)+CO_2(g) \quad (4)$$

and,

$$CaMg(CO_3)_2(s)+2SiO_2(aq) = CaMgSi_2O_6(s)+ 2CO_2(g) \quad (5)$$

As a case study we examine the skarn formation, change in magnetite solubility at the Beni Bou Ifrour skarn-type magnetite deposit in northern Morocco (El Rhazi and Hayashi, 2002). We assumed the following very simple ore-forming process. Primary hydrothermal fluid derived from magmatic water was initially CO_2-free and NaCl-saturated at 300°C (38.0 wt% NaCl). Next, 5 or 10 mol % of CO_2 dissolved into the fluid by reaction with calcite, and then halite precipitated because NaCl solubility lowered to 37.0 or 36.0 wt% NaCl by the addition of CO_2. The drop in Cl^- concentration caused precipitation of magnetite, and the change in magnetite solubility was calculated. Temperature, pH, and redox state are assumed to be constant (300°C, pH=4.5 and pyrite-pyrrhotite-magnetite "PPM" buffer) to evaluate only the effect of elimination of Cl^- by dissolving CO_2. Under these conditions, molalities of $FeCl_n^{2-n}$, one of the dissolved iron species in hydrothermal water, were calculated using equilibrium constants of the following reaction (Ohmoto et al., 1994).

$$3FeCl_n^{2-n} + 4H_2O\ (l) = Fe_3O_4(\text{magnetite}) + 6H^+ + 3nCl^- + H_2\ (aq) \quad (6)$$

From Eqn. (6), K_n, the equilibrium constants of Eqn. (6) for various *ns* (n=0-4) are expressed using pH and activities of dissolved species as follows:

$$\log K_n = 3\log\alpha_{FeCl_n^{2-n}} + 6\text{pH} - 3n\log\alpha_{Cl^-} - \log\alpha_{H_2(aq)} \quad (7)$$

Magnetite solubility, $m_{\text{magnetite}}$, is obtained as a total of molalities obtained from Eqn. (7).

From the calculation by Eqn. (7), 1.070 mol Fe/kgH_2O is dissolved in the initial magnetite-saturated fluid. If 5 mol % and 10 mol % CO_2 added, the concentration of iron species in the solution drops to 1.021 and 0.975 mol Fe/kgH_2O, respectively. That means 5 or 10 mol % CO_2 decreases magnetite solubility by 4.5 or 8.9 % relative to the initial CO_2-free fluid. This calculation suggests that a magnetite-saturated hydrothermal fluid may precipitate ore-scale quantity of magnetite during skarn mineral formation. Skarn mineralization is not a simple process as described here. Changes of pH and/or fluid mixing will more effectively control ore-formation (El Rhazi and Hayashi, 2002). However, this study suggests that elimination of NaCl from hydrothermal fluid by the effect of CO_2 is not a negligible in discussions of the genesis of skarn ore.

4. Conclusions

Synthetic fluid inclusions with compositions of 6-40 wt% NaCl and 5 mol % CO_2 were examined by microthermometric observations, and the halite solubility curve in CO_2-bearing fluid was obtained. This shows that 5 mol % of CO_2 lowers halite solubility by 1 wt%. The halite solubility in 40 wt% NaCl and 5 mol % CO_2 solution agrees with that of Schmidt et al. (1995).

The solubility of magnetite in skarn ore-forming fluid is calculated, and a decrease of it with an effect of decrease in Cl- caused by dissolution of CO_2 is investigated. It suggests that an effect of CO_2 on NaCl solubility is not negligible factor in discussions of behavior of hypersaline aqueous fluid in ore-forming process.

Acknowledgments: We are thankful to H. Nakazawa, T. Kakegawa and K. Tsukamoto for constructive and precise advice. This work was supported by fund from the Ministry of Education, Science, Sports, Culture, and Technology, Japan to K. H. This study was conducted as a part of H. N's doctoral project partly supported by a scholarship of the 21st Century COE program from Tohoku University. We thank N. Takeno, the editor of *Resource Geology*, L. W. Diamond, and an anonymous reviewer for their careful review of the manuscript.

References

Bakker, R. J. (1999) Adaptation of the Bowers and Helgeson (1983) equation of state to the H_2O-CO_2-CH_4-N_2-NaCl system. Chem. Geol., 154, 225–236.

Benrath, A., Gjedebo, F., Schiffers, B. and Wunderlich, H. (1937) Über die Löslichkeit von Salzen und Salzgemischen in Wasser bei Temperaturen oberhalb von 100°. I. Zeitschr. anorg. und alleg. Chemie, 231, 285–297.

Bischoff, J. L. (1991) Densities of liquids and vapors in boiling NaCl-H_2O solutions: a PVTX summary from 300° to 500°C. Amer. Jour. Sci., 291, 309–338.

Bodnar, R. J. (1994) Synthetic fluid inclusions: XII. The system H_2O-NaCl. Experimental determination of the halite liquidus and isochores for a 40 wt% NaCl solution. Geochim. Cosmochim. Acta, 58, 1053–1063.

Bodnar, R. J., Burnham, C. W. and Sterner, S. M. (1985) Synthetic fluid inclusions in natural quartz. III. Determination of phase equilibrium properties in the system H_2O-NaCl to 1000°C and 1500 bars. Geochim. Cosmochim. Acta, 49, 1861–1873.

Bowers, T. S. and Helgeson H. C. (1983) Calculation of the thermodynamic and geochemical consequences of nonideal mixing in the system H_2O-CO_2-NaCl on phase relations in geologic systems: Equation of state for H_2O-CO_2-NaCl fluids at high pressures and temperatures. Geochim. Cosmochim. Acta, 47, 1247–1275.

Chiodini, G., Marini, L. and Russo, M. (2001) Geochemical evidence for the existence of high-temperature hydrothermal brines at Vesuvio volcano, Italy. Geochim. Cosmochim. Acta, 65, 2129–2147.

Chou, I. M. (1987) Phase relations in the system NaCl-KCl-H_2O. III: Solubilities of halite in vapor-saturated liquidus above 445°C and redetermination of phase equilibrium properties in the system NaCl-H_2O to 1000°C and 1500 bars. Geochim. Cosmochim. Acta, 51, 1965–1975.

Diamond, L. W. (1992) Stability of CO_2 clathrate hydrate + CO_2 liquid + aqueous KCl-NaCl solutions: Experimental determination and application to salinity estimates of fluid inclusions. Geochim. Cosmochim. Acta, 56, 273–280.

Duan, Z. and Sun, R. (2003) An improved model calculating CO_2 solubility in pure water and aqueous NaCl solutions from 273 to 533 K and from 0 to 2000 bar. Chem. Geol., 193, 257–271.

Duan, Z., Møller, N. and Weare, J. H. (1995) Equation of state for the NaCl-H_2O-CO_2 system: prediction of phase equilibria and volumetric properties. Geochim. Cosmochim. Acta, 59, 2869–2882.

Dugdale, A. L. and Hagemann, S. G. (2001) The Bronzewing lode-gold deposit, Western Australia: P-T-X evidence for fluid immiscibility caused by cyclic decompression in gold-bearing quartz-veins. Chem. Geol., 173, 59–90.

El Rhazi, M. and Hayashi, K. (2002) Mineralogy, geochemistry, and age constraints on the Beni Bou Ifrour skarn type magnetite deposit, northeastern Morocco. Resource Geol., 52, 25–39.

Frantz, J. D., Zhang, Y.-G., Hickmott, D. D. and Hoering, T. C. (1989) Hydrothermal reactions involving equilibrium between minerals and mixed volatiles: 1. Techniques for experimentally loading and analyzing gases and their application to synthetic fluid inclusions. Chem. Geol., 76, 57–70.

Frantz, J. D., Popp, R. K. and Hoeling, T. C. (1992) The compositional limits of fluid immiscibility in the system H_2O-NaCl-CO_2 as determined with the use of synthetic fluid inclusions in conjunction with mass spectrometry. Chem. Geol., 98, 237–255.

Fu, B., Touret, J. L. R. and Zheng, Y. F. (2001) Fluid inclusions in coesite- bearing eclogites and jadeite quartzite at Shuanghe, Dabie Shan (China). Jour. Metamor. Geol., 19, 531–547.

Genge, M. J., Balme, M. and Jones, A. P. (2001) Salt-bearing fumarole deposits in the summit crater of Oldoinyo Lengai,

Northern Tanzania: interactions between natrocarbonatite lava and meteoric water. Jour. Volcanol. Geotherm. Research, 106, 111–122.

Hanley, J. J., Pettke, T., Mungall, J. E. and Spooner, E. T. C. (2005) The solubility of platinum and gold in NaCl brines at 1.5 kbar, 600 to 800°C: A laser ablation ICP-MS pilot study of synthetic fluid inclusions. Geochim. Cosmochim. Acta, 69, 2593–2611.

Holloway, J. R. and Reese, R. L. (1974) The generation of N_2-CO_2-H_2O fluids for use in hydrothermal experimentation I. Experimental method and equilibrium calculations in the C-O-H-N system. Amer. Mineral., 59, 587–597.

Keevil, N. B. (1942) Vapor pressures of aqueous solutions at high temperatures. Jour. Amer. Chem. Soc., 64, 841–850.

Kelley, D. S. and Früh-green, G. L. (2001) Volatile lines of descent in submarine plutonic environments: Insights from stable isotope and fluid inclusion analyses. Geochim. Cosmochim. Acta, 65, 19, 3325–3346.

Knight, C. L. and Bodnar, R. J. (1989) Synthetic fluid inclusions: IX. Critical properties of NaCl-H_2O solutions. Geochim. Cosmochim. Acta, 53, 3–8.

Kotel'nikov, A. R. and Kotel'nikova, Z. A. (1990) The phase state of the H_2O-CO_2-NaCl system examined from synthetic fluid inclusions in quartz. Geochem. Intern., 27, 11, 55–66.

Krüger, Y. and Diamond, L. W. (2001) Unexpected behavior of fluid inclusions synthesized from silver oxalate and an aqueous NaCl solution. Chem. Geol., 173, 159-177.

Ohmoto, H., Hayashi, K. and Kajisa, Y. (1994) Experimental study of the solubilities of pyrite in NaCl–bearing aqueous solutions at 250-300°C. Geochim. Cosmochim. Acta, 58, 2169–2185.

Potter, R. W., Babcock, R. S. and Brown, D. L. (1977) A new method for determining the solubility of salts in aqueous solutions at elevated temperatures. Jour. Res. U. S. Geol. Survey, 5, 389–395.

Sawaki, T., Sasada, M., Sasaki, M., Tsukimura, K., Hyodo, M., Okabe, T., Uchida, T. and Yagi, M. (1997) Synthetic fluid inclusion logging to measure temperatures and sample fluids in the Kakkonda geothermal field, Japan. Geothermics, 26, 281–303.

Schmidt, C. and Bodnar, R. J. (2000) Synthetic fluid inclusions: XVI. PVTX properties in the system H_2O-NaCl-CO_2 at elevated temperatures, pressures, and salinities. Geochim. Cosmochim. Acta, 64, 3853–3869.

Schmidt, C., Rosso, K. M. and Bodnar, R. J. (1995) Synthetic fluid inclusions: XIII. Experimental determination of PVT properties in the system H_2O + 40 wt% NaCl + 5 mol% CO_2 at elevated temperature and pressure. Geochim. Cosmochim. Acta, 59, 3953–3959.

Shmulovich, K. I. and Graham, C. M. (1999) An experimental study of phase equilibria in the system H_2O-CO_2-NaCl at 800°C and 9 kbar. Contrib. Mineral. Petrol., 136, 247–257.

Shmulovich, K. I. and Plyasunova, N. V. (1993) Phase equilibria in ternary systems formed by H_2O and CO_2 with $CaCl_2$ or NaCl at high T and P. Geochem. Intern., 30, 53–71.

Sourirajan, S. and Kennedy, G. C. (1962) The system H_2O-NaCl at elevated temperatures and pressures. Amer. Jour. Sci., 260, 115–141.

Sterner, S. M. and Bodnar, R. J. (1984) Synthetic fluid inclusions in natural quartz I. Compositional types synthesized and applications to experimental geochemistry. Geochim. Cosmochim. Acta, 48, 2659–2668.

Sterner, S. M. and Bodnar, R. J. (1991) Synthetic fluid inclusions. X: Experimental determination of P-V-T-X properties in the CO_2-H_2O system to 6kb and 700°C. Amer. Jour. Sci., 291, 1–54.

Sterner, S. M., Hall, D. L. and Bodnar, R. J. (1988) Synthetic fluid inclusions: V. Solubility relations in the system NaCl-KCl-H_2O under vapor-saturated conditions. Geochim. Cosmochim. Acta, 52, 989–1005.

Wang, Z., Jiang, N., Wang, Y., Mao, J. and Yang, J. (2004) Genesis of Kanggur gold deposit in eastern Tianshan orogenic belt, NW China: Fluid inclusion and oxygen and hydrogen isotope constraints. Resource Geol., 54, 177–185.

Wagner, W. and Pruß, A. (2002) The IAPWS formulation 1995 for the thermodynamic properties of ordinary water substance for general and scientific use. Jour. Phys. Chem. Ref. Data, 31, 387–535.

Wilkinson, J. J. (2001) Fluid inclusions in hydrothermal ore deposits. Lithos, 55, 229–272.

Zhang, Y-G. and Frantz, J. D. (1987) Determination of the homogenization temperatures and densities of supercritical fluids in the system NaCl-KCl-$CaCl_2$-H_2O using synthetic fluid inclusions. Chem. Geol., 64, 335–350.

(Editorial handling: Naoto TAKENO)